Available online at www.sciencedirect.com

ScienceDirect

Energy Procedia 4 (2011) 3155–3162

Energy Procedia

www.elsevier.com/locate/procedia

GHGT-10

Reactive transport modeling to assess geochemical monitoring for detection of CO_2 intrusion into shallow aquifers

Sven Fahrner[a], Dirk Schaefer[a], Andreas Dahmke[a]**

[a]Department of Applied Geology, Institute of Geosciences, Ludewig-Meyn-Strasse 10, CAU Kiel, Germany

Abstract

The hypothesis is tested if changes in electric conductivity of groundwater (EC) in response to gaseous CO_2 intrusion are sufficient to be detected using probe measurements and geophysical electromagnetic measurements, e.g. airborne electromagnetic measurements. Virtual reactive scenario modelling is used to simulate the effects of the presence of calcite, CO_2 intrusion rates, depth of the aquifer formation, initial salinity of groundwater and CO_2 intrusion time on changes in EC. In all simulations, EC rises rapidly in response to CO_2 intrusion, however in different magnitudes. When calcite is present, EC changes are strong (+1.11 mS/cm after 24 hours of CO_2 intrusion) mainly due to calcite dissolution, whereas in aquifers without calcite changes are very low (+0.02 mS/cm after 24 hours) and close to the resolution range of probes. Increased depth (250 m / 500 m), i.e. higher temperature and pressure, and higher intrusion rates (up to full saturation) result in stronger rises in EC (+5.08 mS/cm in 500 m depth and 100 % saturation), and initial salinity has a negligible influence on changes in EC. Temporally limited CO_2 intrusion leads to EC values close to pre-CO_2-intrusion-levels in the long-term. Measurement resolution of commercial EC probes is sufficient to detect CO_2 intrusion in almost all cases. In terms of geophysical electromagnetic measurements, applications in the field of monitoring saltwater-freshwater interfaces indicate a sufficient measurement resolution to detect changes in all simulations. However, practical limitations are expected due to the dependence of measurement resolutions on the applied measurement devices and site-specific geological settings.

Keywords: groundwater monitoring; reactive modelling; carbon sequestration; CO_2 leakage; Electzric conductivity of groundwater;

1. Introduction

In the course of long-term CO_2 sequestration measures, leakage from the storage formation of CO_2 cannot be ruled out completely. As a consequence, operators of CO_2 injection activities are required to assess the integrity and safety of the storage complex and to detect CO_2 leakage when occurring, based on a monitoring and verification system developed for each individual storage complex. The monitoring plan includes regular monitoring of shallow aquifer formations through which gaseous CO_2 may migrate in case of leakage, as these formations play an important role in the following senses: (1) Groundwater is defined as a subject of protection in the European Union

* Corresponding author. Tel.:+49 (0)431 880 2896; fax:+49 (0)431 880 7606.
E-mail address: fahrner@gpi.uni-kiel.de

doi:10.1016/j.egypro.2011.02.230

Law and thus constant monitoring is required to assure quality (2) Aquifer formations can act as retardation formations, preventing gaseous CO_2 from further upward migration by CO_2 dissolution and potential fixation in minerals (3) Geochemical changes in groundwater chemistry in response to CO_2 intrusion may help to detect CO_2 leakage before it reaches soil or atmosphere.

However, currently well-established groundwater monitoring technologies are mainly borehole-based, i.e. they include the installation of boreholes, the instrumentation with probes and sampling devices, and regular sampling and laboratory analysis activities. They are expensive and their application is from an economic point of view thus limited to monitoring activities which comprise a moderate number of boreholes, as in the field of contaminated sites or pilot CO_2 injection plants. However, large monitoring areas for industrial CO_2 storage projects up to 100 km^2 [1] raise the requirement for alternative monitoring options. Here, it means the identification of alternative monitoring parameters which can be measured without the expensive installation of a huge number of boreholes. Up-to-date publications revealed that in all investigated cases of CO_2 intrusion into aquifers, comprising field, laboratory and modelling studies, the electric conductivity of the groundwater (EC) increased to levels that can be distinguished from baseline levels [2-7]. EC can be measured both borehole-based and applying geophysical non-intrusive electromagnetic measurements, e.g. airborne electromagnetic measurements (AEM). The latter technology has been successfully applied to detect saltwater intrusion into freshwater aquifers [8, 9] and references therein). However, it is not clear yet how electric conductivity changes in response to CO_2 intrusion at various conditions, i.e. variations in depth, CO_2 intrusion rate, mineralogy of the aquifer, and initial groundwater composition.

Table 1: Initial model setup with mineralogical composition of the solid phase (top), and groundwater composition (bottom). (Concentration values for Fe in the range of numerical errors)

Mineral	*Chemical formula*	*Volume fraction (%)*	*References kinetic data*
Quartz	SiO_2	82	[15]
Potassic feldspar	$KAlSi_3O_8$	6	[2]
Kaolinite	$Al_2Si_2O_5(OH)_4$	3	[15]
Oligoclase	$CaAl_2(SiO_4)_2$	2	[2]
Calcite	$CaCO_3$	2	[15]
Goethite	FeO(OH)	2	[15]
Gibbsite	$Al(OH)_3$	1.5	[15]
Illite	$K_{0.6}Mg_{0.25}Al_{2.3}Si_{3.5}O_{10}(OH)_2$	1.5	[2]

Parameter	*Value*	*Unit*
pH	8.791	-
Temperature	25	°C
Pressure	1	bar
Al	$1.192*10^{-7}$	mol kgw^{-1}
C	$4.936*10^{-3}$	mol kgw^{-1}
Ca	$7.185*10^{-5}$	mol kgw^{-1}
Cl	$2.276*10^{-3}$	mol kgw^{-1}
Fe	$(1.373*10^{-14})$	mol kgw^{-1}
K	$6.844*10^{-3}$	mol kgw^{-1}
Na	$3.344*10^{-4}$	mol kgw^{-1}
Si	$6.199*10^{-5}$	mol kgw^{-1}
Ionic Strength	$5.5*10^{-3}$	-

In this study, a 0D batch reactor modelling approach was chosen where a virtual sandy aquifer was created and CO_2 intrusion simulated, incorporating CO_2 dissolution, kinetic mineral dissolution / precipitation, and cation exchange processes. Different scenarios were calculated with variations in the depth of an aquifer, the CO_2 intrusion rate (i.e. various saturation states of the groundwater with respect to gaseous CO_2), the presence or lack of calcite as dominant buffering mineral and different initial salinities of the groundwater. To assess the suitability of EC as monitoring parameter, we investigated the following hypothesis: The electric conductivity of groundwater changes rapidly, with a measurable magnitude, and long-lasting in response to gaseous CO_2 intrusion into the aquifer in all investigated scenarios and is thus a suitable monitoring parameter. Secondly, we aimed at identifying significant parameters for EC development to allow for prediction of changes in EC in scenarios not calculated for this study. Therein, we focused on the role of calcite due to its significance as primary buffer mineral.

2. Methodology

The software PhreeqC v 2.16 [10] was used for all reactive simulations. The virtual initial model setup is depicted in Table 1, where the mineralogical composition of the solid phase and the initial groundwater composition are given. The aquifer formation has a porosity of 25 %. Initially, groundwater is in equilibrium with quartz, potassic feldspar, kaolinite, goethite and calcite (when present), and with atmospheric CO_2 partial pressure ($p(CO_2) = 3.8*10^{-4}$ bar). Total simulation time is 1 year, with time steps of one hour each. The database "wateq4f.dat"

[11] was used as source for geochemical input data and extended for kinetic mineral dissolution rates for all simulated minerals. The applied rate law has been developed by Lasaga et al. [12-14], kinetic data for the minerals are taken from [2] and [15] Kaolinite provides the exchanger sites for cations. The solubility of gaseous CO_2, which dissolves instantly upon intrusion into the aquifer until equilibrium establishment, was calculated using a dissolution model of Duan et al [16], which enables the calculation of CO_2 solubility at different temperatures, pressures and ionic strengths. The electric conductivity of the groundwater (EC) was calculated manually using an approach by Hughes et al. [17], which is based on a model published by Rossum [18] and relies on the Deybe-Hückel-Onsager equation, but is more robust for EC values above ~1,400 µS cm^{-1} (modified Rossum model). Accordingly, the EC values are calculated as composite ionic conductivity of the anions (G_0^-) and cations (G_0^+) in the solution, lessened by a factor representing electropheric and relaxation effects which diminish the mobility of the ions in solution. In our simulations, the values for these effects were less than 1 % of the absolute EC values. Ions with concentrations below 1 µmol kgw^{-1} (kgw = kilogram water) have not been considered in the EC calculations. The EC calculation implies infinite dilution and equivalent ionic conductivities of the ions determined for 25°C.

The developed scenarios are depicted in Table 2. The scenarios are separated in one group where calcite is present (scenarios 1 – 13) and one group where no calcite is present (scenarios 14 – 23). In both groups, the scenario with CO_2 intrusion over the total simulation time and full saturation of the groundwater with respect to gaseous CO_2 at standard conditions have been chosen as base cases. Both groups include simulations with increased salinity (Ionic strength I up to 1), deeper locations of the aquifer (10 m, 250 m, 500 m) and temporally limited CO_2 intrusion time (1 day). Additionally, one scenario was added to each group where the equivalent ionic conductivities (EIC) of the ions were assumed to decrease with each °C by 2 %. To the knowledge of the authors, no EIC values have been published for temperatures below 25°C, but it is generally assumed that they increase by 2 -3 % per °C for temperature above 25°C [19]. In the scenarios regarding the depth location, corrections for temperature and pressure were performed for CO_2 solubility [16] and temperature correction of the logarithmic value of the equilibrium constants $\log(k_{eq})$ of mineral dissolution / precipitation (van't Hoff equation). Pressure correction of $\log(k_{eq})$ has been shown to be negligible in pre-studies for the pressure range considered. Pressure and temperatures at 10 m, 250 m and 500 m were defined assuming a pressure gradient of 1 bar per 10 m (surface pressure of 1 bar) and a temperature gradient of 3 °C per 100 m (surface temperature of 9 °C).

3. Results & Discussion

Rapidity, durability and magnitude of changes in electric conductivity

In Figure 1, electric conductivity changes in the calculated scenarios in comparison to the pre-CO_2-intrusion state are displayed for the time steps T_1=12 h, T_2 = 24 h and T_3 = 1 year after CO_2 intrusion started. Initial EC values are included in Table 2. In general, EC values increase in all cases in response to CO_2 intrusion. Rises are significantly higher within the first 24 hours when calcite is present, where the first sharp increase is followed by a steady but low rise. When calcite is not present, the first sharp increase is significantly lower and of minor importance in comparison to the subsequent constant but slow increase. This pattern is exemplarily depicted in Figure 2 using data of scenario 2 and scenario 14. It is valid for all scenarios except the simulations with limited CO_2 intrusion time where EC values decline after intrusion stopped almost to pre-CO_2 intrusion level (scenarios 12 and 22 in Figure 2).

Table 2: List of calculated scenarios. Chosen base case scenarios (BC) are coloured grey, changed parameters for each scenario in comparison to BC are bold. EC = Electric conductivity, I = Ionic strength, Temp = Temperature, P = Pressure. In scenarios 1 -13, calcite is present, In scenarios 14 – 23 no calcite is present

Scenario	*Initial EC (mS / cm)*	*Initial I (-)*	*Temp (°C)*	*P (bar)*	*Saturation with CO_2 (%)*	*CO_2 Intrusion time (d)*	*EIC value definition*
1	0.69	$5.5*10^{-3}$	25	1	0.038	0	EIC(25°C)
2	0.69	$5.5*10^{-3}$	25	1	100	365	EIC(25°C)
3	1.25	**0.01**	25	1	100	365	EIC(25°C)
4	12.51	**0.1**	25	1	100	365	EIC(25°C)
5	123.53	**1**	25	1	100	365	EIC(25°C)
6	0.77	$5.5*10^{-3}$	**9.3**	**2**	100	365	EIC(25°C)
7	0.73	$5.5*10^{-3}$	**16.5**	**26**	100	365	EIC(25°C)
8	0.70	$5.5*10^{-3}$	**24**	**51**	100	365	EIC(25°C)
9	0.77	$5.5*10^{-3}$	**9.3**	**2**	**10**	365	EIC(25°C)
10	0.73	$5.5*10^{-3}$	**16.5**	**26**	**10**	365	EIC(25°C)
11	0.70	$5.5*10^{-3}$	**24**	**51**	**10**	365	EIC(25°C)
12	0.69	$5.5*10^{-3}$	25	1	100	**1**	EIC(25°C)
13	0.62	$5.5*10^{-3}$	**9.3**	**2**	100	365	**EIC = 0.686*EIC(25°C)**
No calcite present in the following scenarios							
14	0.71	$5.5*10^{-3}$	25	1	100	365	EIC(25°C)
15	123.53	**1**	25	1	100	365	EIC(25°C)
16	0.54	$5.5*10^{-3}$	**9.3**	**2**	100	365	EIC(25°C)
17	0.75	$5.5*10^{-3}$	**16.5**	**26**	100	365	EIC(25°C)
18	0.72	$5.5*10^{-3}$	**24**	**51**	100	365	EIC(25°C)
19	0.54	$5.5*10^{-3}$	**9.3**	**2**	**10**	365	EIC(25°C)
20	0.75	$5.5*10^{-3}$	**16.5**	**26**	**10**	365	EIC(25°C)
21	0.72	$5.5*10^{-3}$	**24**	**51**	**10**	365	EIC(25°C)
22	0.71	$5.5*10^{-3}$	25	1	100	**1**	EIC(25°C)
23	0.64	$5.5*10^{-3}$	**9.3**	**2**	100	365	**EIC = 0.686*EIC(25°C)**

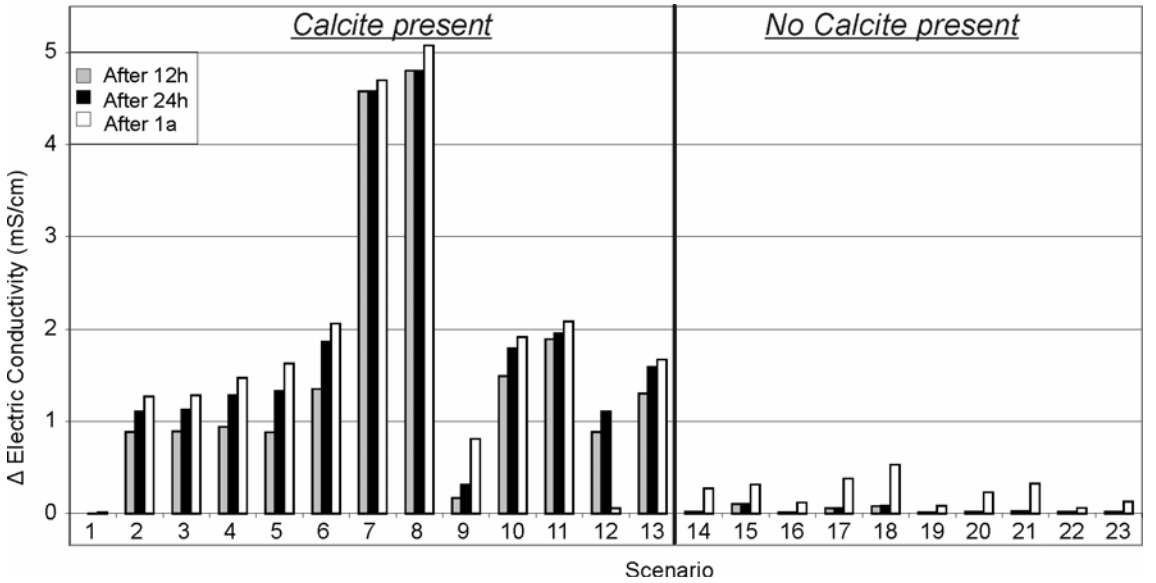

Figure 1: Changes in the electric conductivity of the groundwater in comparison to the pre-CO_2-intrusion state after 12 hours, 24 hours and 1 year for the scenarios listed in Table 2.

Regarding the influence of initial salinity on EC, the relative increases in simulations with high initial salinity (I = 1) are 1.5 % and 0.3 % after one year when calcite is present (S5) and calcite is not present (S15), respectively. With respect to depth (S6-S11, S16-21), the greatest impacts occur from 10 to 250 m (ΔEC(250 m)/ ΔEC(10 m)) at T_1, T_2 and T_3 ranging from 2.3 to 8.9), whereas comparing the scenarios at 500 m to 250 m, the effects are less significant (ΔEC(500 m)/ ΔEC(250 m) at T_1, T_2 and T_3 ranging from 1.0 to 1.4). Nevertheless, the calculation of EC values in different depths includes uncertainties due to expected changes in EIC values with decreasing temperature. A comparison of EC calculations using EIC values at standard conditions (scenarios 6 and 16) and assuming declining EIC values with temperature (scenarios 13 and 23) show a mean decrease of calculated EC values of 16.8 % (standard deviation = 3.4 %, n = 8) from 25 °C to 9.3 °C. In terms of groundwater saturation with respect to CO_2, Figure 3 reveals that EC is strongly dependent on CO_2 saturation when calcite is present and less dependent on CO_2 saturation in a non-calciferous system. EC increases by factors about 2 to 3 from 10 to 100 % saturation in a calciferous system at all three time points, whereas without calcite they increase in maximum by a factor of 1.2 on a lower level.

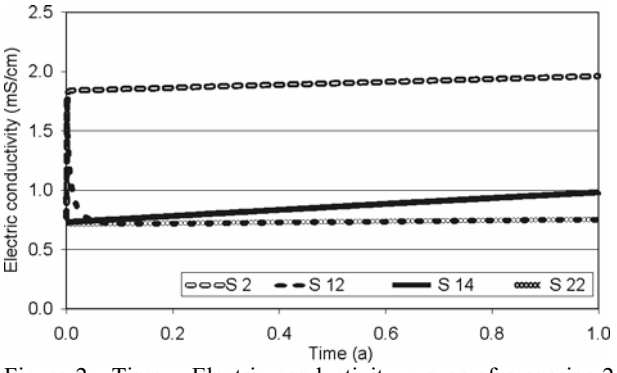

Figure 2: Time – Electric conductivity curves of scenarios 2 and 14 (durable CO_2 intrusion) in comparison to scenarios 12 and 22 (1 day of CO_2 intrusion). See Table 2 for scenario description.

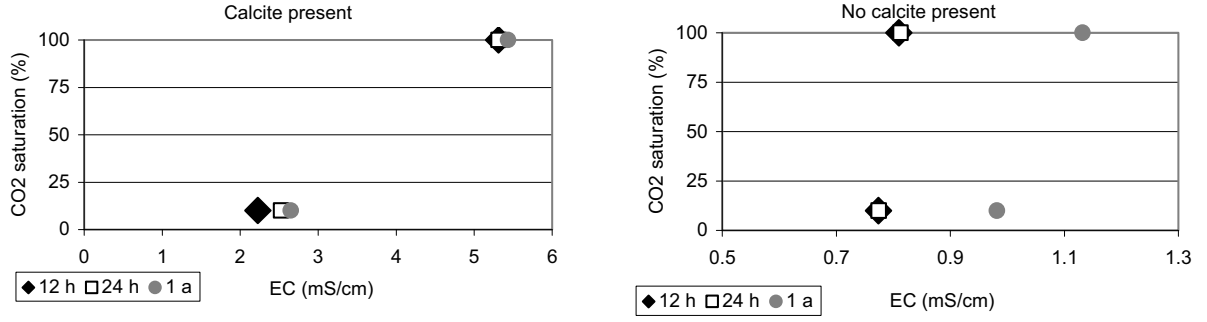

Figure 3: EC values vs CO_2 saturation in 250 m depth for calciferous (S7 / S10) and non-calciferous (S17 / S20) aquifers.

In summary, a rapid reaction (i.e. within the first 24 h after intrusion) is given in all cases. In terms of the magnitude of EC changes, the rapid reaction does not result in strong changes in cases where calcite is not present. Here, the EC values change +0.01 mS/cm in minimum (Scenario 19) and +0.08 mS/cm in maximum (Scenario) after 24 h. After one year EC rises for 0.08 and 0.5 mS/cm, respectively, in these simulations. In terms of magnitude, higher saturation of the groundwater with respect to CO_2, the presence of calcite and increased depth are significant factors which increase the magnitude of changes in EC values. Regarding long-term stability of the induced changes in EC, scenarios with durable CO_2 intrusion can be distinguished from scenarios with temporally CO_2 intrusion. In the first case, the EC values rise further after the first rapid increase, albeit on low levels in scenarios without calcite (Figure 2, scenarios 2 and 14). In the second case EC values decrease almost back to pre-CO_2-intrusion level after 1 year (Figure 2, scenarios 12 and 22), indicating a lack of durability of changes in EC in case of short-term CO_2 intrusion.

Assessment of suitability for monitoring purposes

The measurement resolution of commercial probes for electric conductivity is ~20µS/cm [20]. In using this conventional approach, intrusion of CO_2 could be detected within the first 24 hours after intrusion started in most scenarios, with an exception of low saturation rates in a close-to-surface aquifer without calcite (scenario 19). Also, relatively low increases in comparison to baseline levels, as possible in case of high initial salinity, may be hard to

detect. In terms of detection using electromagnetic measurements, studies investigating saltwater intrusion into freshwater aquifers indicate that existing measurement resolutions can be sufficient to detect the simulated changes in EC. Fittermann [8] conducted resistivity (i.e. reciprocal of conductivity) measurements applying airborne electromagnetic measurement (AEM) to map saltwater intrusion in the Everglades National Park. The attained measurement resolutions (>=0.3 mS/cm) would be sufficient to detect all EC changes after 1 year, and many of them within the first 24 hours. The same resolution has been used by Siemon et al. [9], who monitored coastal aquifers in North-West Germany. These findings give an indication regarding the suitability of EC changes as monitoring parameter, however, measurement resolutions of electromagnetic measurements depend upon the applied technology, calculation approach and geological settings, i.e. porosity of aquifer, electric resistivity of solid phase and stratigraphy. Further research is needed to assess the significance of these parameters in the course of monitoring aquifers at CO_2 storage sites and the limitations of AEM. In addition, further modelling is necessary to define alternative processes which may result in similar changes in EC, but are not due to CO_2 intrusion, e.g. saltwater intrusion.

The significance of the presence of calcite for the development of EC

As calcite presence has been shown to be a major factor with regard to EC-changes, a closer investigation of the processes leading to the results is presented here.

Figure 4 presents the contribution of each ion to the composite ionic conductivities G_0^+ and G_0^- for a scenario with calcite (scenario 6) compared to a scenario without calcite (scenario 16) with otherwise similar conditions (10 m depth, 100 % CO_2 saturation). In the figure, the pre-CO_2 intrusion state (T_0=0h) and the states after 24 h (T_2) and 1 year (T_3) are displayed, values for T_1 = 12 h do not provide additional information and are thus not presented.

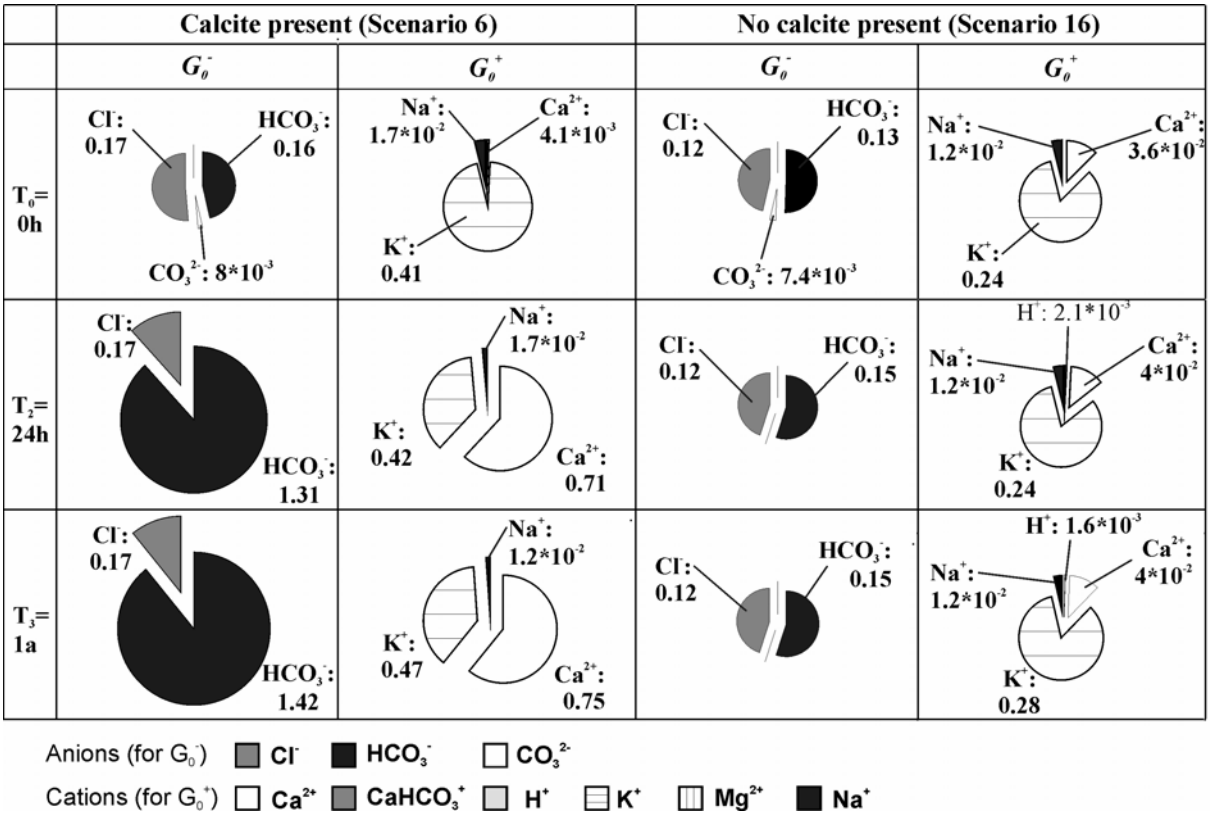

Figure 4: Comparison of the components of electric conductivity (G_0^+, G_0^-) for the scenarios 6, where calcite is present (left) and 16, where no calcite is present (right) at 10 m depth and 100 % CO_2 saturation at T_0 = 0 h, T_2 = 24 h, T_3 = 1 y (from top to down). Numbers give the specific ionic conductivity of each ion (mS/cm), the size of the circle indicates the total values of G_0^+ and G_0^- (see also Figure 1 for total EC values for the respective scenarios).

When calcite is present, major contributions to EC at the initial state come from HCO_3^- and Cl^- on the side of anions and K^+ on the side of cations. After 24 h (T_2), HCO_3^- is the dominating anion with a rapid increase from 0.16 to 1.31 mS/cm, and Ca^{2+} provides the major contribution for G_0^+ due to calcite dissolution. Absolute contributions of the other ions show negligible changes. Up to T_3, slight changes occur mainly in the contributions of K^+ and Na^+ due to slow dissolution of the silicatic minerals, as the groundwater is already saturated with respect to calcite. When no calcite is present, the major contribution to EC before CO_2-intrusion is also provided by K^+, HCO_3^- and Cl^-. In contrast to the calciferous scenario, however, after 24 hours only HCO_3^- shows an increase from 0.13 to 0.15 mS/cm due to the dissolution of gaseous CO_2, whereas all other ions do not change significantly. The slow but steady increase of EC up to T_3, (

Figure 4) is mainly due to a further elevation of the contribution K^+ released via potassic feldspar dissolution.

These findings indicate that at the given model conditions the calcite dissolution is by far the most significant process for elevations of EC in response to CO_2 intrusion via the rapid release of Ca^{2+} and CO_3^{2-} (or HCO_3^- depending on pH). In contrast, the dissolution of gaseous CO_2 and the subsequent production of carbonic acid results in a minor increase of EC, as depicted by the increase of the contribution of HCO_3^- from 0.13 to 0.15 mS/cm in scenario 16 after 24 hours. The low direct influence of gaseous CO_2 dissolution, i.e. the production of ions via carbonic acid production, is due to the fact that the major part carbonic acid does not dissociate due to pH values below the dissociation constant of 6.35.

Limitations of the model setup

The model setup does not regard groundwater flow and thus transport of dissolved species to and from the intrusion site. The interplay between downstream transport of the released species and kinetic dissolution could result in a shift of the respective saturation indices, consequently leading to different dissolution rates and potentially different time-EC-curves. Furthermore, the impact of temperature on EIC values is not quantified, but is important with respect to EC calculations, as shown in the presented simulations. In addition, the impact of a CO_2 gas phase, which could establish in case of higher intrusion rates and excessive CO_2, on the electric conductivity of the formation, could not be assessed. The EC value measured of groundwater measured by probes would not be affected in that case, but geophysical measurements from the surface could deliver divergent signals as gases are rather electric resistors than conductors.

4. Acknowledgements

This study is funded by the German Federal Ministry of Education and Research (BMBF), EnBW Energie Baden-Württemberg AG, E.ON Energie AG, E.ON Ruhrgas AG, RWE Dea AG, Vattenfall Europe Technology Research GmbH, Wintershall Holding AG and Stadtwerke Kiel AG as part of the CO_2-MoPa joint project in the framework of the Special Programme GEOTECHNOLOGIEN.

5. Literature

[1] A. Chadwick, R. Arts, C. Bernstone, F. May, S. Thibeau, P. Zweigel, Best practice for the storage of CO_2 in saline aquifers, in: B.G. Survey (Ed.), Hawthornes, Nottingham, United Kingdom, 2008, pp. 267.

[2] J. Birkholzer, J. Apps, L. Zheng, T. Xu, C.F. Tsang, Research Project on CO_2 Geological Storage and Groundwater Resources: Water Quality Effects Caused by CO_2 Intrusion into Shallow Groundwater, Berkeley, USA, 2008.

[3] S. Carroll, Y. Hao, R. Aines, Geochemical detection of carbon dioxide in dilute aquifers, Geochemical transactions, 10 (2009) 18.

[4] Y.K. Kharaka, J.J. Thordsen, S.D. Hovorka, H.S. Nance, D.R. Cole, T.J. Phelps, K.G. Knauss, Potential environmental issues of CO_2 storage in deep saline aquifers: Geochemical results from the Frio-I Brine Pilot test, Texas, USA, Applied Geochemistry, 24 (2009) 7.

[5] B.R. Strazisar, A.W. Wells, J.R. Diehl, R.W. Hammack, G.A. Veloski, Near-surface monitoring for the ZERT shallow CO_2 injection project, International Journal of Greenhouse Gas Control, 3 (2009) 9.

[6] L. Zheng, J.A. Apps, Y. Zhang, T. Xu, J.T. Birkholzer, On mobilization of lead and arsenic in groundwater

response to CO_2 leakage from deep geological storage, Chemical Geology, 268 (2009) 18.
[7] O.A. de Souza Filho, A.M. Silva, A.Z. Remacre, S.S. Sancevero, A.E. McCafferty, M.M. Perrotta, Using helicopter electromagnetic data to predict groundwater quality in fractured crystalline bedrock in a semi-arid region, Northeast Brazil, Hydrogeology Journal, 18 (2010).
[8] D.V. Fittermann, Geophysical mapping of saltwater intrusion in Everglades National Park, in: Third International Symposium on Ecohydraulics, Salt Lake City, Utah, United States of America, 1999.
[9] B. Siemon, D.G. Eberle, F. Binot, Helicopter-Borne Electromagnetic Investigation of Coastal Aquifers in North-West Germany, Z. geol. Wiss., 32 (2004).
[10] D.L. Parkhurst, C.A.J. Appelo, User's Guide to PhreeqC (Version 2) - A Computer Program for Speciation, Batch Reaction, One-Dimensional Transport, and Inverse Geochemical Calculations, in, Denver, Colorado, 1999.
[11] J.W. Ball, J.W. Nordstrom, D. Kirk, User's manual for WATEQ4F, with revised thermodynamic data base and text cases for calculating speciation of major, trace and redox elements in natural waters, Denver, Colorado, 1991.
[12] A.C. Lasaga, Chemical kinetics of water-rock interaction, Journal of Geophysical Research, 89 (1984) 4009-4025.
[13] A.C. Lasaga, Fundamental approaches in describing mineral dissolution and precipitation rates, in: Chemical Weathering Rates of Silicate Minerals, Mineralogical Soc America, Washington, 1995, pp. 23-86.
[14] A.C. Lasaga, Kinetic theory in the earth sciences, Princeton University Press, Princeton, 1998.
[15] J.L. Palandri, Y.K. Kharaka, A compilation of rate parameters of water-mineral interaction kinetics for application to geochemical modelling, Menlo Park, California, 2004.
[16] Z. Duan, R. Sun, An improved model calculating CO_2 solubility in pure water and aqueous NaCl solutions from 273 to 533K and from 0 to 2000 bar, Chemical Geology, 193 (2003) 15.
[17] S.G. Hughes, E.L. Taylor, P.D. Wentzell, R.F. McCurdy, R.K. Boss, Modelsl for conductance measurements in quality assurance of water analysis, Anal. Chem., 66 (1994) 830-835.
[18] J.R. Rossum, Checking Accuracy of Water Analyses through Use of Conductivity, J. Am. Water Work Assoc., 67 (1975) 204-205.
[19] D.R. Lide, W.M. Hayner, CRC Handbook of Chemistry and Physics - Internet Version 2010, 90th ed., 2010.
[20] WTW, WTW Laboratory products and online instrumentations (http://www.wtw.de/en/index.html), 2010.